

Engineering Report  
Solanis Product Design Challenge  
Inter IIT Tech Meet 12.0

Team 99

December 2023

## Contents

<b>1</b>	<b>Introduction</b>	<b>2</b>
1.1	Abstract of Problem Statement . . . . .	2
1.2	Interpretation of the Problem Statement . . . . .	2
1.3	Aim and Deliverables . . . . .	3
<b>2</b>	<b>Literature Review</b>	<b>3</b>
2.1	Mechanisms for Telescopic Shaft . . . . .	3
2.2	Water Proofing . . . . .	5
2.3	Spark Proofing . . . . .	5
<b>3</b>	<b>Design Process</b>	<b>6</b>
3.1	Preliminary Estimation of Loads . . . . .	6
3.1.1	Preliminary estimation of torsional requirement of rotational motor . . . . .	6
3.1.2	CFD Simulation of Blending . . . . .	7
3.2	Baseline Design . . . . .	8
3.3	Selection of Rotary Motor . . . . .	9
3.4	Selection of Translatory motor . . . . .	10
3.5	Optimization . . . . .	10
3.5.1	Thread Analysis . . . . .	10
3.5.2	Optimizing the Shaft Design . . . . .	11
3.5.3	Bearing Analysis . . . . .	13
3.5.4	Mass-Optimization of Components . . . . .	14
3.6	Material Selection . . . . .	14
3.7	Design of Bellows . . . . .	15
3.8	Sealants . . . . .	17
3.9	Electronics . . . . .	18
<b>4</b>	<b>Stability Analysis</b>	<b>20</b>
4.1	Analysis of Coaxial-Torsional Capability . . . . .	20
4.2	Analysis of Flexural Capability . . . . .	20
<b>5</b>	<b>Portability and Ease of Accessibility</b>	<b>20</b>
5.1	Mass Breakdown . . . . .	21
<b>6</b>	<b>Rendered Images</b>	<b>23</b>
<b>7</b>	<b>Conclusion</b>	<b>23</b>

# 1 Introduction

## 1.1 Abstract of Problem Statement

To design a portable telescopic shaft capable of extending to a depth of 5m and retracting to a length of 1m to be used for application in the blending of solid wastes in slender tanks.

## 1.2 Interpretation of the Problem Statement

To augment the capability and performance of the product in the particular application, the intended functionality of this product was interpreted, summarized findings are provided below,

- In conventional sewage/solid waste storage tanks, the typical ratio of length and diameter is in the range of 1~1.5[4]. To limit the space consumed by these tanks, to address this issue, it is desired to have long or slender tanks. In conventional tanks the blending arises primarily due to axial intermixing(displayed in Fig-1). In the case of tangential intermixing, it requires higher rotational speeds to achieve equivalent mixing performance. In slender tanks, axial intermixing will be ineffective as the extent of the flow field will not be able to effectively cover the entire depth of the tank. Due to the small clearance between the walls and the impeller blades, radial intermixing will be ineffective.

To address this issue our product is designed to undergo **decoupled translatory and rotary motion**. The rotary motion allows for axial mixing regardless of the extent of the axial flow field and the translator motion allows the impeller to cover up to the desired depth, effectively enhancing the global axial flow field.

- Due to ambiguity regarding the constituent materials in waste tanks, the following assumptions are made. The solid waste could be volatile and could ignite due to agitation induced by the impeller. The solid waste is predominantly granular. For design, the slurry is treated as dense to account for resistance to impeller motion and low viscosity to account for penetration into narrow openings in the shaft. Due to the close clearance between the wall and the shafts and impellers, the shear stress generated due to the relative shearing of fluids of walls is to be accounted for.
- All material selection and structural design are based on engineering reasons and no unwarranted constraint is imposed on engineering decisions. The design is optimized and curated for the desired functionality with goals of minimizing lifting weight, sufficing structural safety requirements and elevating functional performance(mixing, portability).

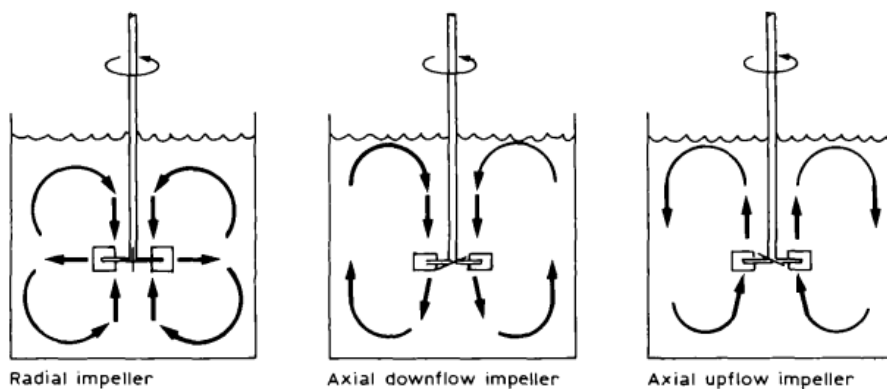


Figure 1: Types of Flow rotating impellers in conventional tanks, taken from [2]

### 1.3 Aim and Deliverables

- Smooth and Reliable Extension: The shaft should be able to smoothly and reliably extend to the full depth of 5 meters.
- Controlled Retraction: The mechanism should allow the shaft to retract to a depth of 1 meter in a controlled manner.
- Light Weight: The design should prioritize lightweight without compromising structural integrity.
- Ease of Operation: Preferably, the mechanism should be single-button controlled for user-friendly operation.
- Water and Spark-Proofing: Incorporate measures to ensure water and spark-proofing for safety and durability.
- Portability: Design the mechanism to be easily portable for enhanced versatility and usability.

## 2 Literature Review

### 2.1 Mechanisms for Telescopic Shaft

A telescopic mechanism is a system that allows the extension and retraction of an object or structure, typically in a linear manner. The basic principle involves the use of components that slide or move within one another, allowing for an adjustable length. Telescopic mechanisms find applications in various fields, such as engineering, automotive, aerospace, and furniture design. Some of the most common telescopic mechanisms are as follows:

#### Pulley and Belt-Driven Mechanism

**Principle:** Utilizes a system of pulleys and belts to transmit motion and extend or retract the telescopic components.

#### Pros:

- Cost-Effective: Pulley and belt mechanisms are often more affordable to manufacture compared to some other types.
- Smooth Operation: They can provide relatively smooth and quiet operation, making them suitable for applications where noise is a concern.
- Simple Design: The design is straightforward, making it easier to implement and maintain.

#### Cons:

- Limited Load Capacity: Pulley and belt systems may have limitations in terms of the amount of load they can effectively handle.
- Slippage: Belts may slip over time, especially in high-torque applications, leading to a decrease in efficiency.
- Wear and Tear: Belts can wear out over time, requiring regular replacement and maintenance.

## Pneumatic/Hydraulic Mechanism

**Principle:** Involves the use of pressurized air (pneumatic) or fluid (hydraulic) to extend and retract the telescopic components.

### Pros:

- High Load Capacity: Pneumatic and hydraulic systems can handle substantial loads, making them suitable for heavy-duty applications.
- Smooth Motion: They provide smooth and controlled motion, crucial for precision applications.
- Variable Speed: Adjusting the pressure allows for variable speeds in extension and retraction.

### Cons:

- Potential Leaks: Hydraulic systems, in particular, are susceptible to fluid leaks, which can be environmentally hazardous and require maintenance.
- Temperature Sensitivity: Performance can be affected by temperature variations, and extreme temperatures may cause issues.
- Complex Maintenance: Repairs and maintenance can be more complex and require specialized knowledge.

## Screw and Motor Driven Mechanism

**Principle:** Utilizes a screw mechanism, often powered by an electric motor, to drive the extension and retraction of the telescopic parts.

### Pros:

- Precise Control: Screw mechanisms can offer precise control over the extension and retraction, making them suitable for applications requiring accuracy.
- High Torque: They can handle high torque loads, making them suitable for heavy-duty applications.
- Versatility: Screw mechanisms can be adapted for various applications and configurations.

### Cons:

- Limited Speed: In some cases, screw-driven mechanisms may have limitations in terms of speed, especially in comparison to hydraulic systems.
- Mechanical Wear: The screw threads can experience wear over time, affecting the long-term reliability of the mechanism.
- Complexity: The system can be more complex than other types, requiring careful design and maintenance.

## Scissor Mechanism

**Principle:** Involves a series of interconnected scissor-like bars that extend and retract in a folding or unfolding motion.

### Pros:

- Compact when Retracted: Scissor mechanisms can collapse into a compact form, making them suitable for applications with limited space.

- Stability: The interconnected scissor structure provides stability during extension and retraction.
- Ease of Integration: They can be integrated into various designs and applications.

### **Cons:**

- Limited Extension Range: Scissor mechanisms often have a limited extension range compared to other types.
- Complex Design: The interconnected nature of scissor mechanisms can make them more complex to design and manufacture.
- Maintenance Challenges: The complexity of the design may lead to challenges in maintenance and repairs.

## **2.2 Water Proofing**

Waterproofing in slurry stirrer mechanisms is of paramount importance due to the challenging environments they operate in, particularly in sludge tanks where water, often contaminated with dirt and sewage, is omnipresent. Effective waterproofing prevents potential electric shock hazards by safeguarding electrical components from water ingress. In environments with high levels of contaminants, such as dirt and sewage, waterproofing acts as a protective barrier, preserving the functionality and longevity of the slurry stirrer. Furthermore, it plays a crucial role in preventing corrosion and rusting of metal components, which are susceptible to damage in the presence of water. Maintaining the electrical integrity of the stirrer mechanism is essential for preventing short circuits and ensuring reliable performance while also contributing significantly to the extension of the equipment's lifespan. Mechanical components, including bearings and gears, benefit from waterproofing as it reduces wear and damage, leading to lower maintenance requirements.

Various common waterproofing methods are employed across diverse industries to shield equipment, structures, and surfaces from the deleterious effects of water. Sealants and caulk, like silicone and polyurethane, are commonly applied to joints and gaps, creating an impermeable barrier. Waterproof membranes, thin layers applied to surfaces, are prevalent in roofing systems and foundations to prevent water penetration. Bituminous coatings, relying on bitumen-based compounds, serve as thick, waterproof layers commonly used in basements and concrete structures. Cementitious waterproofing, involving a cement-based mixture, is ideal for applications like concrete structures, swimming pools, and water tanks. Liquid applied membranes, forming seamless barriers when cured, are versatile for construction applications. Polyurethane waterproofing utilizes coatings that provide resilience and flexibility, suitable for roofs and balconies. Epoxy sealants and coatings create impermeable barriers in industrial settings like flooring and pipes. Geotextiles, permeable fabrics enhance soil stability and drainage in civil engineering projects. Water-repellent treatments, applied to surfaces, reduce water absorption while allowing vapour to pass through. Grout and joint sealants are used to fill gaps, preventing water penetration in bathrooms, kitchens, and exterior structures. Additionally, for underwater waterproofing, specialized solutions like below-grade waterproofing materials are utilized to ensure the durability and effectiveness of structures submerged in water. These diverse methods cater to specific needs, with considerations such as application type, environmental conditions, substrate materials, and budget constraints guiding the selection of the most suitable and effective waterproofing solution.

## **2.3 Spark Proofing**

In the context of slurry mixing operations, particularly in industries dealing with metals, the potential release of methane gas adds an additional layer of complexity and risk. Methane, a highly flammable and explosive gas, is often present in mines, oil refineries, and certain metal processing facilities. The act of mixing slurry, which involves combining solid particles with a liquid medium, can disturb the

surroundings and release trapped gasses, including methane. The environment for the current application is, therefore a methane-rich environment, and this needs to be taken into account while choosing materials and designing parts.

Sparking, a phenomenon frequently observed in the context of ferrous metals, poses a significant risk, especially in environments prone to ignition, such as mines, oil refineries, gas stations, and methane gas plants. The sparks, generated through friction or impact against metal surfaces, can lead to catastrophic consequences. To mitigate this danger, non-sparking metals are employed.

Common examples of non-sparking metals include copper and copper-based alloys. Copper-aluminium alloys also fall within this category due to their ability to resist sparking. The exceptional thermal and electrical properties of these non-sparking metals play a crucial role in preventing spark formation, thereby reducing the potential for hazardous incidents. Additionally, non-metals like plastic and acrylic are inherently non-sparking.

However, non-sparking metals, particularly copper and its alloys, exhibit drawbacks such as softness and high electrical conductivity. These limitations restrict their load-carrying capacity and elevate the risk of electric shocks. In response to these challenges, viable alternatives are Chlorinated Poly Vinyl Chloride (CPVC) and Acrylonitrile Butadiene Styrene (ABS), plastics with commendable strength and non-sparking characteristics. These polymers not only avoid the risks associated with sparking but also serve as a robust electric insulator.

### 3 Design Process

#### 3.1 Preliminary Estimation of Loads

The limit case of structural design for the assembly arises in the following states.

- For rotation of the impeller, the member is suspended into the tank and the shaft is in it's fully stretched position(as the effective thickness of individual shafts in the assembly will be least and the hydrodynamic pressure acting on the impeller is highest).
- During translation against gravity the shaft undergoing relative motion is confined by the contact with the above shaft which behaves rigidly, in this configuration the torsional stress acting on the particular shaft is maximum.

##### 3.1.1 Preliminary estimation of torsional requirement of rotational motor

As the end shaft is decoupled with the impeller, the rotation of the impeller, will not generate any first-order forces in the shaft. The loads acting on the impeller are mentioned below

- Contribution of hydrodynamic pressure acting on the faces of the impeller.
- Contribution of shear stresses exerted by relative motion between wall and impeller(depicted in Fig-2).
- Contribution of shear stresses exerted due to intermixing/blending.

The hydrodynamic pressure could be investigated by theoretical expressions for variation of pressure along depth. For design, the depth is assumed as  $5m$ . The preliminary design dimensions for impeller are presented in Table-1. <sup>1</sup>. The contribution of shear stress is estimated through numerical simulation, the details are reported in the following subsection.

---

<sup>1</sup>To achieve effective intermixing the net radial protrusion must lie between  $D/4$  and  $2D/3$  [2], to account for solids settling near walls the radial protrusion is enhanced but the protrusion from the shaft is kept within limits

Impeller	Dimensions	Remark
Width of each blade	50mm	
Depth of each blade	50mm	
Radial Protrusion	150mm <sup>1</sup>	Will effectively dictate the mixing performance of the system
Number of Blades	3	

Table 1: Preliminary Dimensions of Impeller

### 3.1.2 CFD Simulation of Blending

A two-fluid model for rheology of the slurry is considered. The eulerian equations are presented below

$$\frac{\partial \alpha_s \rho_s}{\partial t} + \nabla \cdot (\alpha_s \rho_s \vec{u}_s) = 0 \quad (1)$$

$$\frac{\partial \alpha_s \rho_s \vec{u}_s}{\partial t} + \nabla \cdot (\alpha_s \rho_s \vec{u}_s \vec{u}_s) = -\alpha_s \nabla p + \nabla \cdot (2\alpha_s \mu_c \eta_r \mathbf{D}_d \pm \vec{F}_k \mp \vec{F}_L) \quad (2)$$

$$\frac{\partial \alpha_l \rho_l \vec{u}_l}{\partial t} + \nabla \cdot (\alpha_l \rho_l \vec{u}_l \vec{u}_l) = -\alpha_l \nabla p + \nabla \cdot (2\alpha_l \mu_c \eta_r \mathbf{D}_d - \nabla \cdot (u_l) \mathbf{I}/3) \mp \vec{F}_k \pm \vec{F}_L \quad (3)$$

Eq. 1 - continuity equation for the granular phase, eq. 2 - momentum equation for the granular phase, and eq. 3 - momentum equation for the liquid phase, Here the notations are based on Ansys Fluent Manual[1].

To account for the solid phases, the relative suspension viscosity is scaled as per equation-4 [3].

$$\eta_{sus} = \eta_c (1 + 2.5\phi/\phi_m) \quad (4)$$

The suspension viscosity and yield stress were obtained from empirical relations published in literature [7]. The slurry is designed for intermixing an effective total suspended solid concentration of 2%. And the density is conservatively estimated as  $1200\text{kg/m}^3$ .

The simulation is presented by considering a 2-D unit planar section and using this simulation, the mixing performance is also assessed. A pictorial description of the geometry is presented in Fig-??.

The qualitative mixing performance was assessed through a segregated simulation, where the mixing homogeneity is qualitatively estimated through equation-5

$$H(t) = 1 - \frac{\text{StandardDev}(\text{Massfraction}(t))}{\text{StandardDev}(\text{Massfraction}(t = 0))} \quad (5)$$

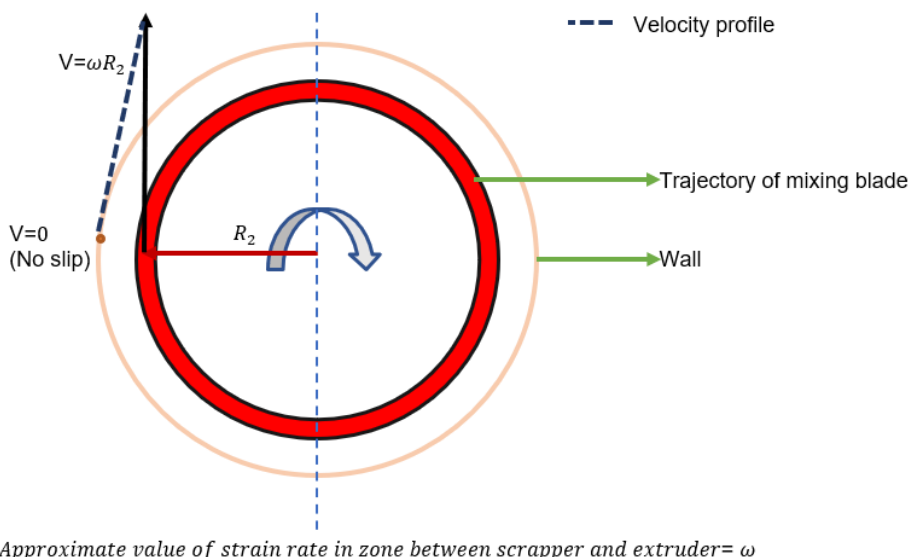


Figure 2: Depiction of shear-induced by relative motion of wall and impeller

Rotational speed [rpm]	30	60	90	120
Torque contribution due to hydrodynamic pressure(5m)[Nm]	48.9	48.9	48.9	48.9
Torque contribution due to motion between walls and impeller[Nm]	0.015	0.1	0.25	0.5
Torque contribution due to mixing[Nm]				
Cummulative Torque[Nm]	48.915	49	49.15	49.4

Table 2: Initial estimate of torque requirements of motor

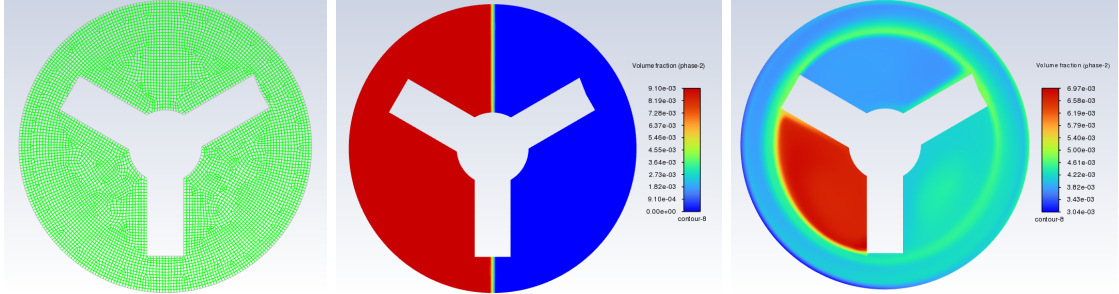


Figure 3: (a) Mesh Geometry of Blending Simulation, (b) Initial Condition for assessing mixing performance( $H=0$ ), (c)End state of simulation for 200RPM( $H=80\$$ )

It is to be noted that the mixing performance in this case is **not equivalent** to the blending performance but can give a qualitative estimate of the blending performance. The time taken for mixing performance of 90% is designated as mixing time in this work. The temporal variation of mixing homogeneity for the particular shaft at varying rotational speeds is plotted in Fig-5

ID	Maximum Torque required for positive translation through corresponding shaft
Shaft-1	7.3
Shaft-2	6.5
Shaft-3	5.9
Shaft-4	5.3
Shaft-5	3.8
Shaft-6	3.3
Shaft-end-with impeller	0.0

Table 3: Torsional Requirements of the translatory motor

### 3.2 Baseline Design

In the first design iteration, our team embarked on developing a novel threaded shaft mechanism featuring internal and external threads. The primary goals were to achieve translational and rotational motion using two decoupled motors while adhering to given constraints, such as extension limits and the minimum inner diameter dictated by the rotor motor.

**Mechanism Description:** Our design incorporates threaded shafts with both internal and external threads. Two motors drive the system independently:

- **Translational Motor:** Responsible for unscrewing the threads, causing shaft expansion and retraction.
- **Rotary Motor:** Located at the end of the last shaft, rotates the impeller for mixing purposes.

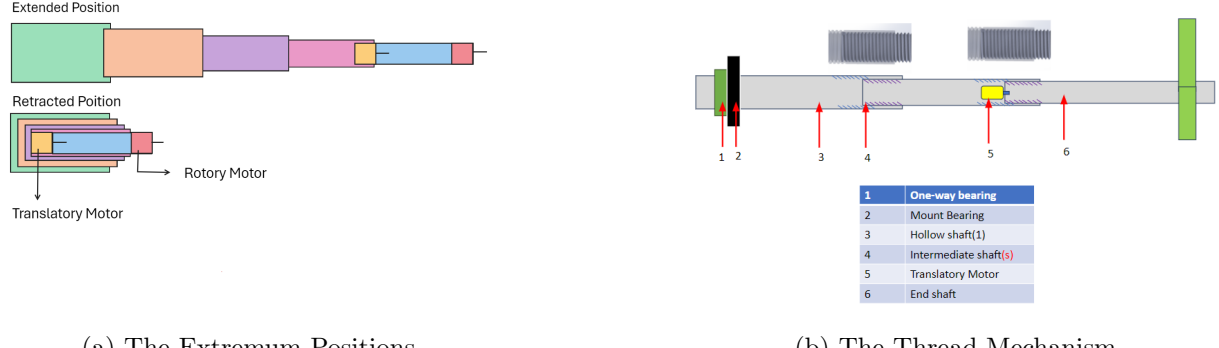


Figure 4: Conceptual Design

**Thread Design:** Threads were selected to prevent slippage due to self-weight, ensuring stability during operation. An arbitrary thickness of 10 mm was applied, providing structural integrity and supporting the overall functionality of the system.

**Conservative Design Approach:** The initial design was intentionally conservative, focusing on meeting the minimum criteria outlined in the problem statement. This allowed us to establish a baseline understanding of the system's capabilities.

**Constraints:** The design faced two critical constraints:

- **Extension Limits:** The system needed to operate within specified extension limits, dictating the range of motion achievable by the translational motor.
- **Rotor Motor Diameter:** The diameter of the rotor motor imposed a minimum criterion on the inner diameter of the inner shaft, influencing the overall dimensions of the system.

Table 4: Shaft Dimensions and Threads - Baseline Design

Shaft	Length (m)	External Diameter (mm)	Internal Diameter (mm)	Internal Thread	External Thread	Internal Thread Length Description (Top to Bottom)
6	0.9	125	165	-	M 165 x 6	Top Offset 100 Thread 800 Bottom Offset 0
5	0.9	165	200	M 165 x 6	M 200 x 8	Top Offset 100 Thread 800 Bottom Offset 0
4	0.9	200	250	M 200 x 8	M 250 x 8	Top Offset 100 Thread 800 Bottom Offset 0
3	0.9	250	300	M 250 x 8	M 300 x 8	Top Offset 100 Thread 800 Bottom Offset 0
2	0.9	300	350	M 300 x 8	M 350 x 6	Top Offset 100 Thread 800 Bottom Offset 0
1	1.0	350	400	M 350 x 6	-	Top Offset 200 Thread 800 Bottom Offset 0

### Results and Findings:

- The conservative design successfully met the specified constraints.
- Preliminary tests indicated satisfactory translational and rotational motion within the prescribed limits.
- Despite meeting initial constraints, opportunities for optimization were identified to enhance cost-effectiveness and efficiency.
- The primary areas for optimization include adjusting the thickness of each shaft, modifying thread dimensions, and optimizing the length of individual shafts, particularly considering their varying diameters. A longer shaft with a smaller diameter is ideally preferred to minimize mass.

### 3.3 Selection of Rotary Motor

Based on cumulative torsional requirements of torsional motor, and considering a safety factor of 1.5, a Nema 34 motor (with 1:15 gearbox) of capacity 75KNm. The product is commercially available [5]. The weight of the motor is around 5.8Kg. Based on the provided torque charts, the impeller can effectively operate till 75rpm.

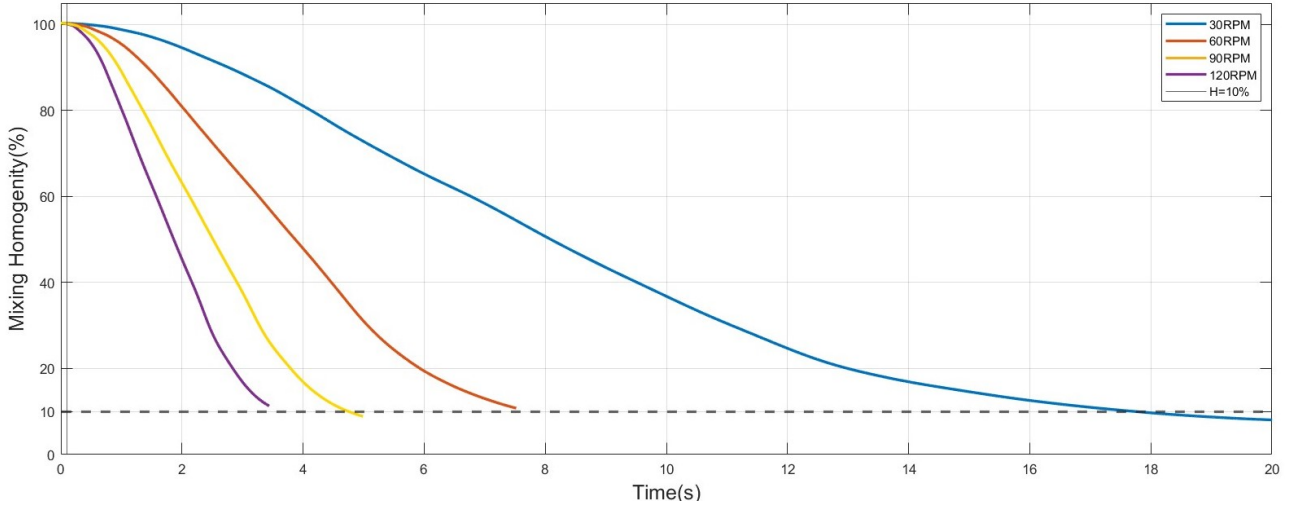


Figure 5: Temporal Variation of Mixing Homogeneity at varying rotational speeds

### 3.4 Selection of Translatory motor

The pitch of the threads is designed to avoid slip (acting as a passive gravity retention system) and to allow efficient transfer of rotary into torsional motion; for positive vertical translation, the shaft bears against the above rigid shaft, and the entire weight has to be translated, the numerical value of torsional requirement was theoretically solved using energy conservation and was later validated through numerical simulation. The torsional requirements for translating through each shaft is presented in Table 3. Based on these requirements, a commercially available NEMA 34 motor of capacity 85Kg-cm is opted for[6]

### 3.5 Optimization

#### 3.5.1 Thread Analysis

Power screws serve as mechanical components for converting rotary motion to linear motion and vice versa. Comprising a threaded shaft (screw) and a nut with corresponding threads, the screw's rotation propels it through the nut, resulting in linear motion. In our design, the nut is also a threaded shaft.

$$\text{Area of contact } A = \frac{\pi}{4} (D^2 - d^2) \cos(\lambda)$$

$$\text{Normal Force } F_{\text{square}} = F \cos(\alpha)$$

$$\text{Shear Force } F_{\text{square}} = F \sin(\alpha)$$

$\alpha$  is the contact angle,

$\lambda$  is the lead angle,

$D$  is the major diameter,

$d$  is the minor diameter.

For square threads,  $\alpha = 0$  degrees, and for ACME threads,  $\alpha = 14.5$  degrees.

Due to their efficient power transmission and precise motion control, power screws find widespread use in industrial and mechanical systems, making them a fitting choice for our mechanism. Unlike V threads, power screws are designed to minimize resistance between the screw and the nut. For optimal power transmission, screws with trapezoidal threads or smaller thread angles are recommended. Power threads typically come in two main types: square and ISO metric trapezoidal.

Table 5: Square Threads Analysis

Parameters	Shaft 1	Shaft 2	Shaft 3	Shaft 4	Shaft 5
Load it should support (N)	154.92	141.58	128.71	116.30	104.37
Normal Force (N)	154.92	141.58	128.71	116.30	104.37
Shear Force (N)	0	0	0	0	0
Internal diameter (mm)	145	140	135	130	125
Major diameter (mm)	146	141	136	131	126
Minor Diameter (mm)	139	134	129	124	119
Mean Diameter	142.5	137.5	132.5	127.5	122.5
Lead angle (degrees)	1.92	1.99	2.06	2.15	2.23
Area of Contact (mm <sup>2</sup> )	1565.20	1510.21	1455.23	1400.24	1345.25
Per one lead length					
Normal Stress (MPa)	0.10	0.09	0.09	0.08	0.08
Shear Stress (MPa)	0.00	0.00	0.00	0.00	0.00

In our application, we conducted an analysis of both thread types, and either square or ISO metric trapezoidal threads proved suitable. The operational differences between the two were negligible. After several iterations, we finalized the thread parameters with a pitch of 4 mm, shaft thickness of 5 mm, and a lead of 15 mm. These specifications were chosen to optimize the performance of our power screw mechanism.

Table 6: ACME Threads Analysis

Parameters	Shaft 1	Shaft 2	Shaft 3	Shaft 4	Shaft 5
Load it should support (N)	154.92	141.58	128.71	116.30	104.37
Normal Force (N)	149.98	137.07	124.61	112.60	101.04
Shear Force (N)	38.79	35.45	32.23	29.12	26.13
Internal diameter (mm)	145	140	135	130	125
Major diameter (mm)	146	141	136	131	126
Minor Diameter (mm)	139	134	129	124	119
Mean Diameter	142.5	137.5	132.5	127.5	122.5
Lead angle (degrees)	33.84	34.79	35.79	36.85	37.95
Area of Contact (mm <sup>2</sup> )	1300.77	1240.96	1181.14	1121.33	1061.58
Per one lead length					
Normal Stress (MPa)	0.12	0.11	0.11	0.10	0.10
Shear Stress (MPa)	0.03	0.03	0.03	0.03	0.02

### 3.5.2 Optimizing the Shaft Design

In the refinement of our design, several crucial considerations and optimizations were undertaken to ensure the robustness and functionality of the threaded mechanism. Once the pitch was conclusively set at 4 mm, careful attention was directed towards determining the appropriate thickness of the shaft. Ultimately, a thickness of 5 mm was chosen, striking a balance between structural stability and operational efficiency.

One critical aspect that demanded meticulous attention was the depth of cut or extrusion for the chosen thread type, be it Square or ACME. It was judiciously decided that the depth of cut or extrusion should equate to half the pitch. This decision not only adhered to the principles of sound mechanical design but also contributed to the overall efficiency of the power screw mechanism.

To further fortify the structural integrity of the shafts, it was imperative to prevent any overlap between internal and external threads. This meticulous consideration, while seemingly subtle, plays

a pivotal role in ensuring the longevity and reliability of the entire mechanism.

Upon finalizing these parameters, our focus shifted to addressing the issue of excess length in the fully retracted position, which initially extended to 1.4 meters. This posed a challenge that required a meticulous reevaluation of the individual shaft lengths. Through a systematic reconfiguration, we were able to optimize the lengths to eliminate the extraneous 0.4 meters in the retracted position, achieving a more streamlined and efficient design.

Table 7: Shaft Dimensions and Characteristics

Shaft	Length (m)	Internal Diameter (mm)	External Diameter (mm)	Volume (m <sup>3</sup> )
7	0.4	120	125	0.00038465
6	0.6	125	130	0.000600525
5	0.7	130	135	0.0007280875
4	0.8	135	140	0.0008635
3	0.9	140	145	0.0010067625
2	1	145	150	0.001157875
1	1	150	155	0.001197125

Table 8: Thread Length Descriptions

Top Offset (m)	Thread (m)	Bottom Offset (m)
<b>Internal Thread</b>		
-	-	-
0.1	0.4	0.1
0.05	0.6	0.05
0.05	0.7	0.05
0.05	0.8	0.05
0.1	0.85	0.05
0	0.9	0.1
<b>External Thread</b>		
0	0	0
0	0.1	0
0	0.05	0
0	0.05	0
0	0.05	0
0	0.05	0
-	-	-

An additional nuance emerged during the evaluation of the assembly process. It was identified that potential wear and tear of threads, particularly concerning the internal ones with offsets at both the top and bottom, could occur during the insertion of the lower diameter shaft with external threads. To preemptively mitigate this concern, a deliberate taper of 1 mm was introduced at the bottom section. This not only facilitated a smoother assembly process but also safeguarded against any inadvertent damage to the threads, enhancing the overall reliability and longevity of the power screw mechanism.

For the optimized Shaft, the torsional requirement for Translation changed as mentioned in -Tables 9 and 10.

In Section 3.7, we detailed the incorporation of bellows for waterproofing the mechanism, a crucial feature to protect the internal components from environmental factors. The decision to include bellows necessitated a modification in the design of shaft 7, where a section of the shaft needed to protrude for the attachment of the bellows.

The use of bellows is instrumental in safeguarding the internal components, particularly the shafts,

Table 9: Square Threads Analysis -  $\mu = 0.4$

Inputs	Shaft 1	Shaft 2	Shaft-3	Shaft-4	Shaft-5	Shaft 6
T_r (Nm)	4.608	4.069	3.571	3.110	2.687	2.330
T_l (Nm)	4.379	3.860	3.380	2.938	2.532	2.191
Mean Diameter (mm)	145	140	135	130	125	120
Coefficient of Friction	0.4	0.4	0.4	0.4	0.4	0.4
Pitch (mm)	4	4	4	4	4	4
Load it should support (N)	154.92	141.58	128.71	116.30	104.37	94.176

Table 10: Square Threads Analysis -  $\mu = 0.5$

Inputs	Shaft 1	Shaft 2	Shaft 3	Shaft 4	Shaft 5	Shaft 6
T_r (Nm)	5.74	5.07	4.45	3.87	3.35	2.90
T_l (Nm)	5.49	4.84	4.24	3.69	3.18	2.75
Mean Diameter (mm)	145.00	140.00	135.00	130.00	125.00	120.00
Coefficient of Friction	0.50	0.50	0.50	0.50	0.50	0.50
Pitch (mm)	4.00	4.00	4.00	4.00	4.00	4.00
Load it should support (N)	154.92	141.58	128.71	116.30	104.37	94.18

from water and other external elements. These flexible, accordion-like structures create a protective barrier, preventing water ingress and ensuring the integrity of the internal mechanisms. The waterproofing mechanism with bellows is essential for applications in environments where exposure to liquids, such as water or chemicals, is a concern.

The inclusion of bellows, however, introduced a design consideration regarding shaft 7. To accommodate the attachment of bellows, it became necessary to modify the length of shaft 7. This adjustment ensures that the bellows can be securely attached to the protruded section of the shaft, providing effective waterproofing without compromising the overall functionality of the system.

The decision to modify the shaft length is a trade-off between maintaining the waterproofing integrity and ensuring the smooth operation of the telescopic assembly. By detailing this modification in the subsequent table, we address the specific alterations made to shaft 7 to seamlessly integrate the bellows into the design.

Table 11: Final Shaft Dimensions and Characteristics

Shaft 7	Shaft 6	Shaft 5	Shaft 4	Shaft 3	Shaft 2	Shaft 1	
Length (m)	0.7	0.65	0.7	0.75	0.8	0.9	0.9
Internal Diameter (mm)	120	125	130	135	140	145	150
External Diameter (mm)	125	130	135	140	145	150	155

### 3.5.3 Bearing Analysis

The primary objective is to optimize the design of a bearing that plays a pivotal role in supporting an entire shaft within our telescopic mechanism. The emphasis lies in tailoring the bearing to withstand significant axial loading, a critical consideration for the efficient functioning of the machinery.

Several key parameters were systematically adjusted during the analysis to ascertain their impact on the bearing's performance. These parameters include the inner diameter (ID), the number of balls, outer diameter (OD), pitch diameter, and ball width. By manipulating these variables, we sought to identify the most effective combination for our specific application.

Axial loading takes center stage in our optimization efforts due to its pronounced influence on the bearing's operational stability. Given the higher magnitude of axial loading in our case, the design iterations were particularly focused on ensuring the bearing's robustness under these challenging conditions.

Our optimization strategy involved a systematic and iterative approach. For a fixed inner diameter, various combinations of the number of balls, outer diameter, pitch diameter, and ball width were explored. Each iteration aimed to fine-tune the bearing parameters, considering factors such as load-bearing capacity, durability, and friction to arrive at an optimal design.

$$P = \frac{C}{(P_d \cdot W) + \frac{P_r}{R}}$$

Where:

$P$  : Axial load

$C$  : Basic dynamic load rating

$P_d$  : Dynamic equivalent axial load

$W$  : Load distribution factor

$P_r$  : Equivalent radial load

$R$  : Equivalent radius of curvature



Figure 6: Custom Fabricated One-way Bearing Mount

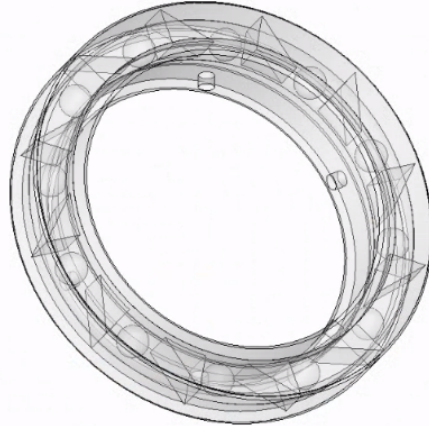


Figure 7: One-way Bearing Mount- Internal Section

### 3.5.4 Mass-Optimization of Components

To enhance the portability of the system, the mass of several parts was reduced by adjusting the dimensions upon structural optimization studies. All custom components were mass-optimized. Snippets of various optimization studies is presented in Fig-8

## 3.6 Material Selection

In the initial stages of our design process, we began by considering the use of aluminum for our setup, taking into account the need for threads, sufficient thickness to incorporate internal and external threads, and the inclusion of an oil hole for self-lubrication of metal threads. However, after a thorough literature review, it became evident that proceeding with metals posed significant drawbacks,

such as increased weight, susceptibility to electric shocks, and the necessity for additional shockproofing mechanisms.

Subsequently, we shifted our focus to composite materials. Considering the initial load estimates, a composite structure emerged as a viable and robust option for our application. We opted for a ply layup configuration of  $0/90/90/0/\pm 45/\pm 45/0/90/90/0$  to compensate for both radial (pressure) and axial loads (weight of the assembly).

Another material under consideration was CPVC (Chlorinated Polyvinyl Chloride). It exhibited the necessary strength to withstand the load conditions with a comfortable Factor of Safety (FOS). Moreover, CPVC had a lower density ( $1.52 - 1.56 \text{ g/cm}^3$ ) compared to CFRP (Carbon Fiber Reinforced Polymer) composite at 60% Fiber Volume Fraction, which had a density of approximately  $1.6 \text{ g/cm}^3$ . The subsequent design iterations incorporated CPVC as our main shaft material, given its thermal stability, machinability into tubes, and straightforward manufacturing process.

In addition to CPVC, we explored the use of ABS (Acrylonitrile Butadiene Styrene), which is 3D printable. The low density of ABS ( $1.05 - 1.15 \text{ g/cm}^3$ ) further contributed to the reduction of overall mass in comparison to other polymers.

Both CPVC and ABS were selected for their low moisture-absorbing capacity, a crucial characteristic for our application. The bearings were crafted from aluminum, while mounts and the impeller were 3D printed using PEEK (Polyether Ether Ketone). The decision to use PEEK was based on its ease of 3D printability and suitability for the required shapes.

Aluminium was chosen for handles and rollers in our design due to its low coefficient of friction and ease of manufacturing. This comprehensive material selection process ensures that each component is tailored to its specific function while collectively contributing to the overall efficiency and reliability of the system.

### 3.7 Design of Bellows

Sealing mechanisms commonly employed today are unsuitable for threaded pipes due to the presence of both translational and rotational movements, making them susceptible to damage. To address the need for seals that can withstand these complex motions and protect against slurry leakage, a solution is proposed involving the utilization of flexible rubber bellows. The proposed design addresses the challenge of lateral pressure increment with depth, a common occurrence as the depth increases. The flexible rubber bellows are strategically attached to the base and the last shaft, aiming to prevent water leakage and ensure spark proofing.

The choice of a flexible rubber bellows is justified by its ability to expand and compress in accordance with the height of the telescopic shaft. With the slurry density considered, the pressure at a depth of 5 meters is calculated to be 50 Kpa. The bellows selected for the design demonstrate the capability to withstand this pressure, considering factors such as nominal diameter, number of turns, and length. Through online research, it was determined that utilizing four bellows, each with

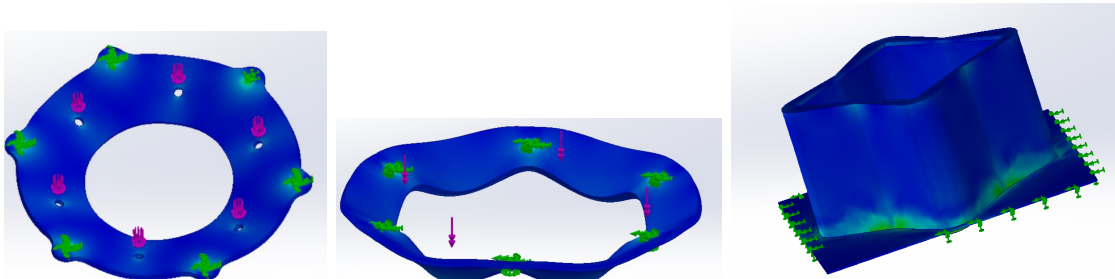


Figure 8: Snippets from Optimization Studies(Material-ABS)

PROPERTY	ASTM TEST	PEEK	
		UNFILLED	30% GLASS FILLED
PHYSICAL			
Water Absorption, immersion 24 hours (%)	D-570	0.5	0.11
MECHANICAL			
Tensile Strength (psi)	D-638	14,000	24,620
Flexural Modulus (psi)	D-790	590,000	1,450,000
Izod Impact, notched (ft-lbs/in of notch)	D-256	1.6	1.84

Figure 9: PEEK Mechanical Properties

PROPERTY	ASTM or UL Test	ABS	
		PHYSICAL	
Density (lb/in <sup>3</sup> ) (g/cm <sup>3</sup> )			
Density (lb/in <sup>3</sup> )	D792	0.038	
(g/cm <sup>3</sup> )		1.04	
Water Absorption, 24 hrs (%)			
Water Absorption, 24 hrs (%)	D570	-	
MECHANICAL			
Tensile Strength (psi)	D638	6,500	
Tensile Modulus (psi)	D638	340,000	
Tensile Elongation at Break (%)	D638	25	
Flexural Strength (psi)	D790	11,000	
Flexural Modulus (psi)	D790	320,000	
Compressive Strength (psi)	D695	-	
Compressive Modulus (psi)	D695	-	
Hardness, Rockwell	D785	R105	

Figure 10: ABS Mechanical Properties

its compression factor, combined with separate ring structures, would enhance the overall performance.

The specific bellows chosen for the design can expand to 1400 mm and retract to 250 mm when compressed. The design comprises three bellows of 1400 mm and one rubber bellow capable of expanding to 800 mm and contracting to 150 mm. While these bellows are custom-made, their dimensional characteristics align with industry standards, featuring an inner diameter of 160 mm and a thickness of 0.5 mm. Extensive simulations have confirmed the resilience of these bellows under pressure, ensuring they remain intact during the insertion process.

Calculations were conducted to determine the shear stress values at the ends of the 5m setup. The obtained total circumferential stress is 9.22 MPa, while the longitudinal stress is 4.62 MPa, each in distinct principal directions. The primary material constituting our rubber bellow is neoprene, a chloroprene-based rubber, augmented with additional polymers to bolster its strength properties. Neoprene rubber typically exhibits a tensile strength of 20 MPa.

Consequently, taking this into account, our minimum safety factor stands at 2.16. Importantly, it is worth noting that this safety factor is a baseline value that will be further augmented with the inclusion of other materials such as NBR and Hypalon. These additional materials aim to enhance the physical properties of the rubber bellow without altering its compression ratio.

The rubber bellow system is designed to accommodate sudden impact load conditions, and in this context, the design impact strength is set at half of the actual yield strength. Given that the rubber used operates within the elastic region, this assumption remains valid. Consequently, the minimum design impact strength is established at 10 MPa. The radial stress experienced at the outer surface of the bellow is an order of magnitude lower than the design impact strength, registering at 0.1 MPa. This ensures that the bellow can effectively withstand any abrupt impact resulting from slurry motion. Additionally, the shafts play a crucial role in providing support to the bellow under pressure impacts. The incorporation of an extra 100mm in length is a proactive measure to account for potential bending of the bellow without risking tearing or compromising the system's integrity. This comprehensive approach ensures resilience against sudden impacts and enhances the overall robustness of the rubber bellow system.

The expansion rate of the bellows aligns with the translational speed of the shafts (i.e 900mm/min), ensuring smooth and synchronized movements. The assembly sequence involves the sequential expansion of the bellows, with the first, second, and third bellows reaching 1400 mm, followed by the final bellow expanding to 800 mm from a contracted position of 150 mm. The ring structures, crucial components in this design, are fabricated using ABS PC, a material selected for its ability to withstand

pressure and facilitate interconnection between bellows. Notably, the chosen material is 3D printable, offering a weight advantage over traditional aluminium structures.

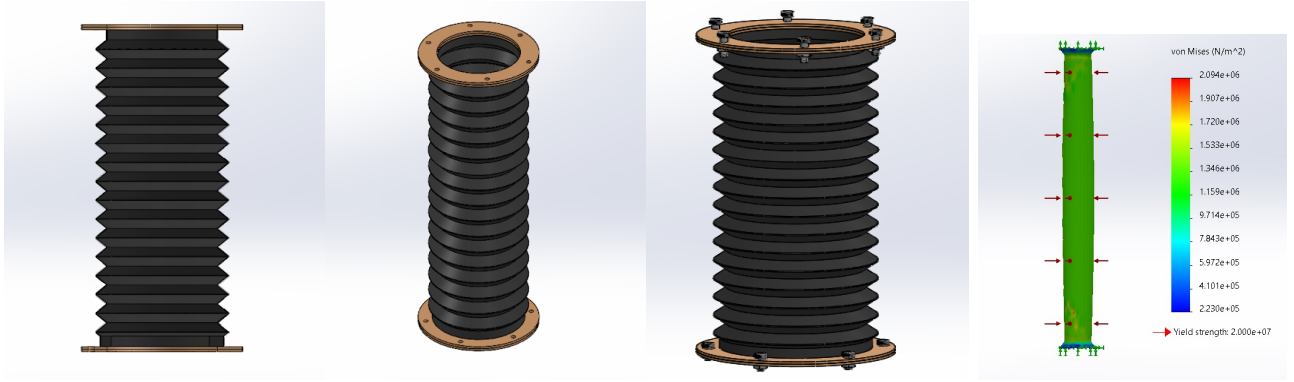


Figure 11: Bellows-CAD and Numerical Simulation

To enhance the seal and prevent water leakage into the system, M10 bolts with a length of 20 mm, along with hex sealing bolts of the same pitch (1.5 mm), are employed. These sealing nuts and bolts, sourced from McMaster, contribute to the fully retractable and compressible nature of the bellows model, ensuring it meets the stringent requirements for pressure resistance and load-bearing capabilities.



Figure 12: O-ring based Bolt and Nut(for sealing)

### 3.8 Sealants

Another design consideration incorporated is the inclusion of bellows to prevent direct contact of the telescopic tubes to the methane environment. The details of the mechanism are discussed forthwith. The bellows are expandable and designed to withstand pressure. Even if a spark is generated the blocking of contact with methane will eliminate any case of inflammation.

There are mainly three points of leakage that may arise. The main locations are:

- At the threaded sections between two telescopic tubes.
- At the attachment point of the bellow to the shaft at the lower end.
- At the interface between the shaft and the impeller.

The widely used method for sealing the gaps between threads and arresting any leakage is the use of teflon tapes or specialized adhesives. These are applied on the outer threads and used majorly in

non - heavy duty applications like plumbing. This is clearly not a solution especially when the liquid is a slurry mixture. Plus there is a chance of the slurry sticking inside the threads. To overcome this problem we have incorporated bellows as described below. The presence of bellows eliminates all contact of the slurry to the shafts and prevents leakage.



Figure 13: Sealant Integrated Ball Bearing(to be custom-fabricated)

The bellow is attached to the shaft at both ends with the help of bolts and nuts which have inbuilt O-rings that prevent leakage. However, there exists a relative rotary motion of the bellow at the lower section which may cause leaking. To prevent this, we have come up with a new mechanism. We make use of a combination of O-rings and ball bearings to inhibit any sort of leakage at the point of attachment of the bellow. The O-ring is attached to the shaft and the ball bearing is fitted on this O-ring to give a tight fit. The bellow is then attached on top of the ball bearing with the help of bolts. We are using Chemical-Resistant Super-Resilient Viton, Fluoroelastomer O-Rings and Flanged Ultra-Thin Ball Bearings to achieve this. It is important to note that this is a unique combination given the fact that we are aiming to eliminate all sorts of leakages.

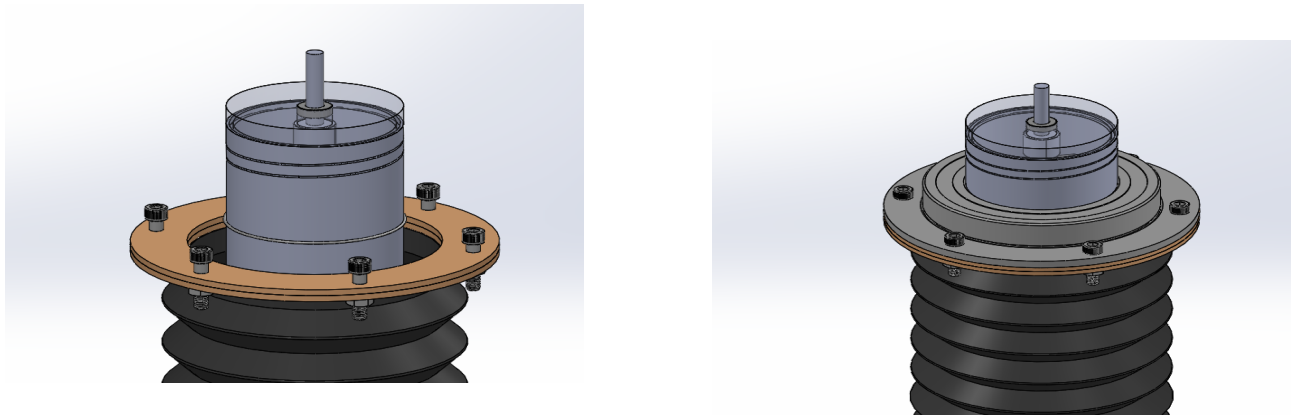


Figure 14: End connection of Bellow

In pump applications, the commonly used method of preventing leakages at the point of contact between the rotating shaft and the impeller is the use of spring loaded rotary shaft seals. There are majorly two types of seals available, single seals and double seals. Double seals make use of an additional fluid layer to prevent leakage. However, since they have complex installations and use external fluid for their working, we are going ahead with single seals. We are using Spring-Loaded Rotary Shaft Seals that would be fitted at the junction to prevent any leakage.

### 3.9 Electronics

The electronic subsystem of the proposed mechanism has been meticulously designed for optimal user-friendliness, accessibility, and reliability. Its modular architecture, independent of other subsystems,

ensures straightforward maintenance and facilitates seamless upgrades. The versatile control options offer flexibility, supporting both manual onboard operation and remote control via the integrated LoRa antenna, boasting an impressive range of 800 meters. This antenna can also be connected to the PCB, extending the control range and enabling operation status display on other devices.

Powering the electronic subsystem is a 24 V rechargeable battery with a capacity of 20,000 mAh, enhancing the system's portability and sustainability. Its detachable and reattachable feature adds versatility, allowing for convenient maintenance and adjustments. The inclusion of the battery introduces a weight of 3 kg into the electronics system.

Streamlined into a single PCB, the electronics exhibit a simplified circuitry design, optimizing operational efficiency. Three prominent LEDs act as status indicators, with red signaling ongoing operations, green denoting a standstill, and yellow indicating leaks within the bellows for enhanced safety measures. User interaction is facilitated through four main buttons, each serving a distinct purpose.

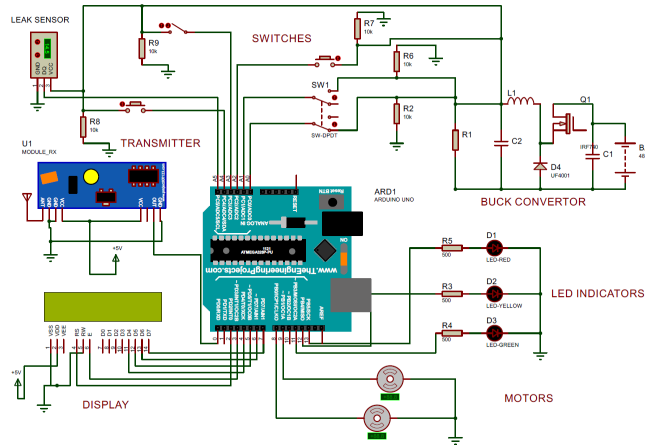


Figure 15: Electronics Boc Schematic

The first button initiates translation to a depth of 5 meters, the second ensures the sole rotation of the impeller, and the third orchestrates both the translation of the telescopic mechanism and the rotation of the impeller. A fourth emergency stop button is incorporated for immediate halting of all motion, prioritizing safety in unforeseen circumstances.

To enhance system reliability, a rotation adapter is strategically positioned near the top of the electronic box, mitigating potential issues arising from wire entanglement during relative motion between wires and shafts. The PCB plays a central role in the system, encompassing a stepper motor controller tailored for NEMA 34 motor models and integrating necessary microcontroller components. Provisions for a separate charging connector to recharge the battery and a 6-pin connector for electronic component connections to both the stepper motors and the leak sensor have been made.

A standout feature is the incorporation of a strategically positioned leak sensor (SOS ASM Leak Sensor R-1) near the top mount, addressing potential bellow failure or tearing. Buck converters in the PCB design ensure voltage division meets the specific requirements of individual components.

In addition to versatile control options, the electronic subsystem includes buttons on both the electronic box and the remote control. This dual control interface provides redundancy and flexibility, allowing operators to control the mechanism from either location. The seamless integration of a remote control option significantly expands the application scope of the mechanism, making it suitable for diverse environments and operational scenarios.

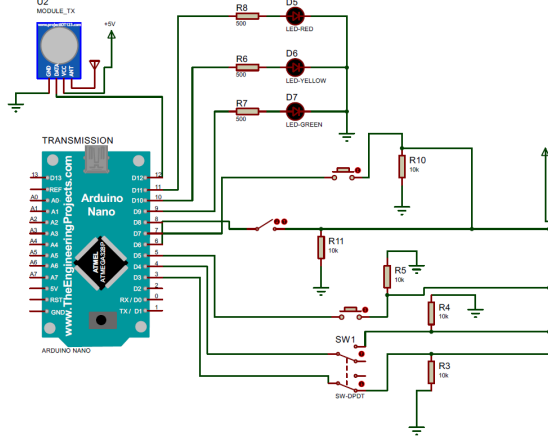


Figure 16: Remote Control Schematic

## 4 Stability Analysis

### 4.1 Analysis of Coaxial-Torsional Capability

During the positive translation, the below shafts bear on the shaft just above it and the axial load too has to be accounted. Based on theoretical results the torsional deformation and stress pattern is calculated and is verified through numerical simulation. The results are presented in Table-???

ID	$\tau$ (KPa)	Max axial stress (KPa)	Von-Mises Stress	FoS-ABS	Angular Defromation(Rad)	Axial Deformation (mm)	Abs Def (mm)
Shaft-1	78.3	169.8	217.3	207.1	0.0004	0.0642	0.0707
Shaft-2	35.6	163.2	174.5	257.9	0.0002	0.0617	0.0632
Shaft-3	21.7	156.6	161.0	279.4	0.0001	0.0526	0.0531
Shaft-4	14.9	151.3	153.5	293.2	0.0001	0.0477	0.0479
Shaft-5	7.2	74.8	75.8	593.7	0.0000	0.0220	0.0221
Shaft-6	5.0	68.1	68.7	655.5	0.0000	0.0186	0.0187
Shaft-end	0.0	121.4	121.4	370.6	0.0000	0.0357	0.0357

Table 12: Torsional Design of Shafts

### 4.2 Analysis of Flexural Capability

Courtesy of the high flexibility of the chosen material(ABS) for the shafts, the flexural rigidity of the material is highly compromised,

- In its fully stretched position(5m), the one-point flexural stiffness is numerically calculated to be 0.23KN/m. A representative image of the simulation is presented in Fig-20
- In its fully compressed position(1m), the one-point flexural stiffness is numerically calculated to be 62.73KN/m. A representative image of the simulation is presented in Fig-20

The flexural capacity in the compressed state at which it will be transported can be considered sufficient.

## 5 Portability and Ease of Accessibility

The total assembly comes in two versions, depending on the material used for the shafts. With ABS pipes, the system weighs 31.14 kg, while CPVC increases the mass to 35.23 kg. Given that the mass

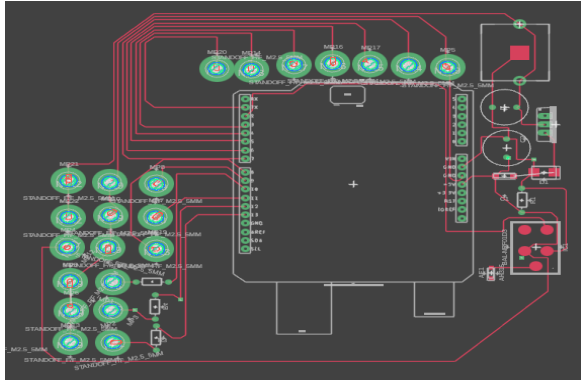


Figure 17: PCB Routing

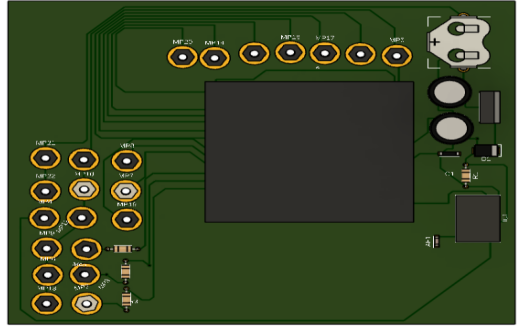


Figure 18: Top View

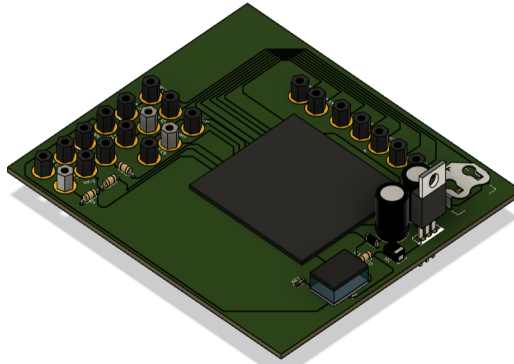


Figure 19: Isometric View

exceeds 25 kg, we utilize ball transfer rollers for easy movement within the workspace. These rollers, equipped with four balls each, ensure smooth maneuverability.

Strategically positioned handles enhance the ease of lifting and positioning during setup or relocation. The roller setup is 3D printed with PEEK material, using recessed flange mount ball transfers mounted directly to a 3D-printed roller block. A simple screw locking mechanism holds it in place, and the top handle ensures firm and smooth motion.

For portability, the mixer has a retractable design, compacting its dimensions to 1 meter. Though not explicitly designed for carrying, this feature enhances storage efficiency and ease of transport when not in use. The combination of ball transfer rollers, ergonomic handles, and a retractable design underscores the user-centric approach, emphasizing functionality and practicality.

For terrain applications and overhead tanks, a separate one-strap backpack model is incorporated. A handlebar on the lid facilitates easy lifting. This model allows charging the battery compartment independently, reducing the mass burden when carrying through challenging terrains. The backpack comes with provisions to hold the impeller securely through a push-lock mechanism, and a connector powers other electronic components.

## 5.1 Mass Breakdown

The total weight of the assembly is around 31.1Kg, with a detachable mass of 4.6Kg. Provisions for integrating roller into the system is provided. The weight breakdown is presented in Table-13

The comprehensive design prioritizes both portability and accessibility, recognizing their pivotal roles in ensuring practical usability. The overall weight of 31.1 kg strikes a balance between sturdiness and maneuverability. Cylindrical rollers strategically positioned enable effortless movement within workspaces, complemented by ergonomically designed handles for ease of lifting and positioning during setup or relocation.

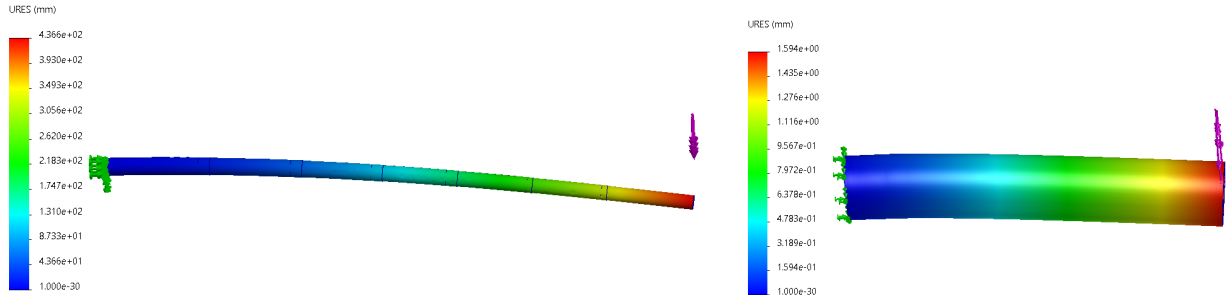


Figure 20: Simulation of one-point lateral bending in (a) Stretched Configuration (b) Unstretched Configuration

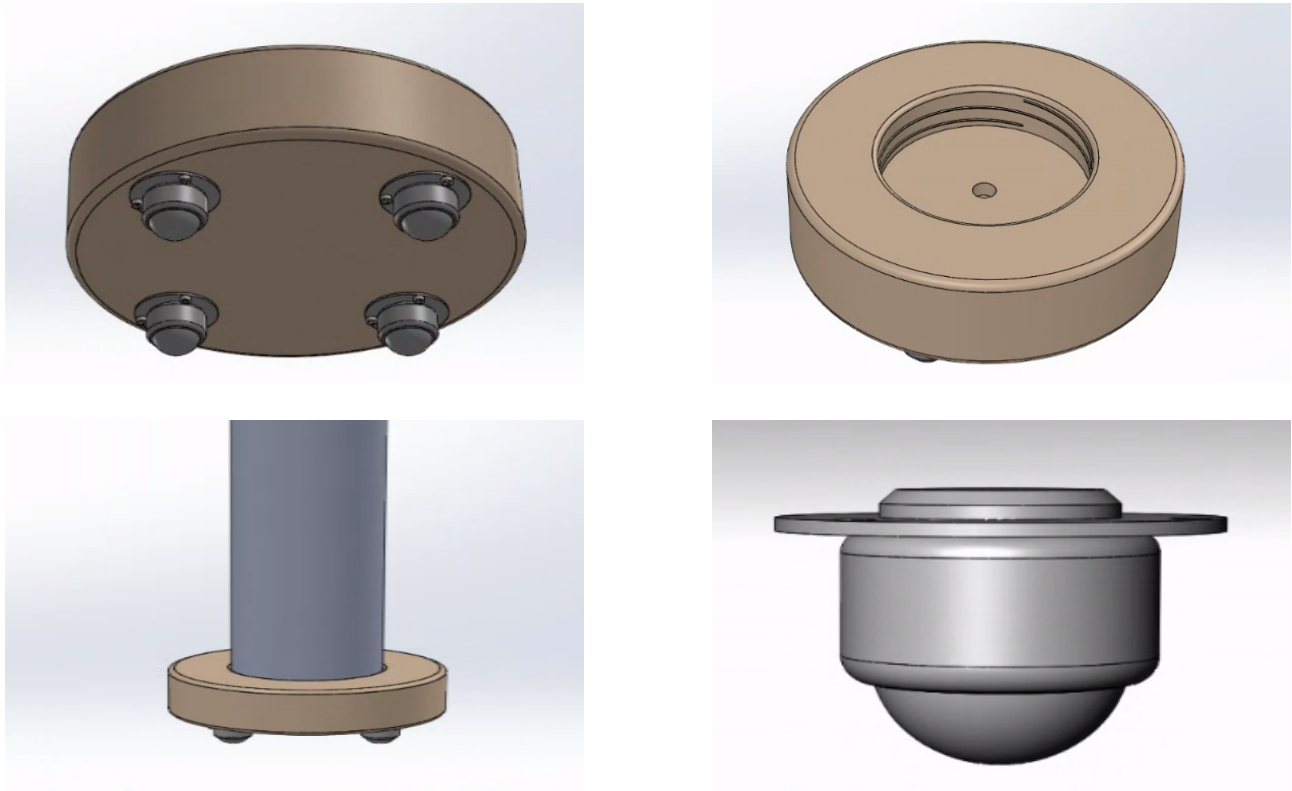


Figure 21: Roller Provisions for Easy Portability

The retractable design further enhances portability, compacting the mixer's dimensions to 1 meter. This combination of features underscores a user-centric approach, emphasizing both functionality and practicality in diverse operational scenarios.

In conclusion, the mixer is not only portable and compatible but can also navigate different terrains, ensuring versatility and ease of use in various environments.

S.No	Component	Weight(Kg)
1	Lithium E-Battery	3
2	Casing and Boards	1.6
	<b>Detachable Weight</b>	<b>4.6</b>
3	Enclosing architectural shell with plate	1.5
4	Handles	0.24
5	One-way bearing mount	0.75
6	Impeller	0.96
7	Rotary motor	3.3
8	Gear Box	2.5
9	Translatory motor	3.3
10	Weight of shaft	8.1
11	Weight of bellow setup	4.9
12	Sundries	0.9
	<b>Lift Weight</b>	<b>26.5</b>
	<b>Total Weight</b>	<b>31.1</b>

Table 13: Weight Breakdown of Assembly

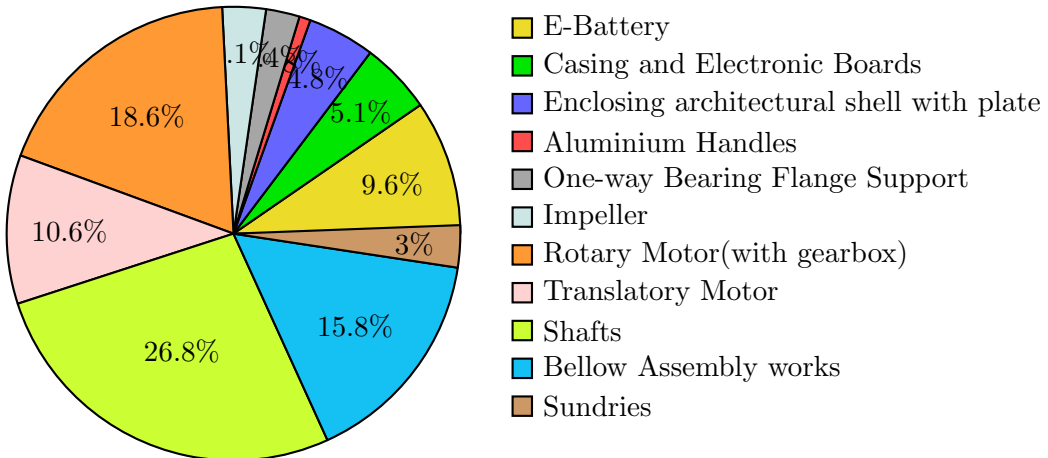


Figure 22: Breakdown of costs

## 6 Rendered Images

Rendered Images of the assembly is presented in Figures-23,24,26,27,28,29,30. The aforementioned images showcase the CAD model of the assembly. To better elucidate the features of design most rendered images are shown in compressed condition.

## 7 Conclusion

In conclusion, our design has not only met but surpassed the rigorous criteria set by the challenge. The meticulous attention to detail is evident in our solution's leak-proof, spark-proof, and shock-proof features, where the strategic use of CPVC ensures both resilience and safety. The portable nature of our design, coupled with easy handling, reflects a commitment to user convenience. Additionally, the modular electronic subsystem, decoupled for adaptability, and remote control functionality showcase our forward-thinking approach in meeting contemporary technological expectations.

Furthermore, our innovative bellow model has proven highly effective in preventing leaks, enhancing both environmental safety and the longevity of the system. Rigorous Computational Fluid Dynamics (CFD) testing has yielded excellent results, affirming the efficiency of our design under various operating conditions. The impressive number of cycles achieved with our chosen battery type

not only attests to the sustainability of our solution but also emphasizes its cost-effectiveness. In summary, our comprehensive design not only fulfills the designated requirements but positions our solution as a technologically advanced, reliable, and durable answer to the challenges presented by the design task.



Figure 23: Front-View of Assembly-Compressed



Figure 24: Section-View of Assembly-Compressed



Figure 25: Front-View of Assembly-Extended



Figure 26: Front-View of Assembly-Compressed with roller



Figure 27: Section-View of Assembly-Compressed with roller

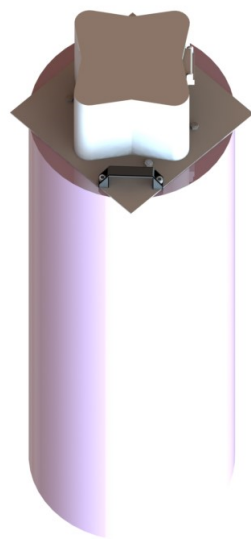


Figure 28: Mounting Configuration(on the tank)



Figure 29: Detachable Electronic Box

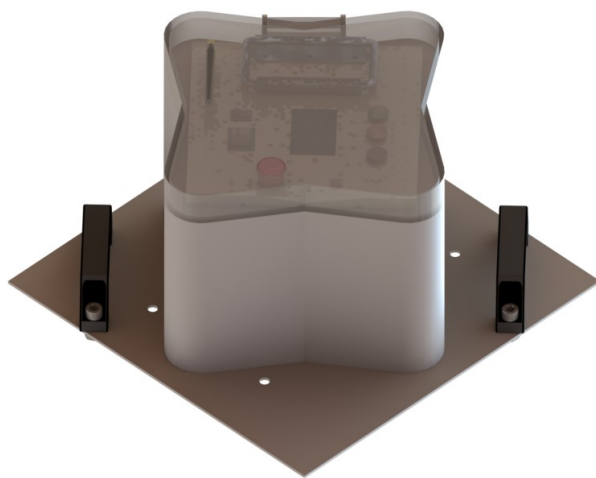


Figure 30: Casing Mount for detachable electrical box

## References

- [1] UDF Ansys FLUENT 12.0 Manual. “ANSYS FLUENT 12.0”. In: *Theory Guide* (2009), p. 67.
- [2] T.R. Cumby. “Slurry mixing with impellers: Part 1, theory and previous research”. In: *Journal of Agricultural Engineering Research* 45 (1990), pp. 157–173. ISSN: 0021-8634. DOI: [https://doi.org/10.1016/S0021-8634\(05\)80147-7](https://doi.org/10.1016/S0021-8634(05)80147-7). URL: <https://www.sciencedirect.com/science/article/pii/S0021863405801477>.
- [3] Irvin M. Krieger and Thomas J. Dougherty. “A Mechanism for Non-Newtonian Flow in Suspensions of Rigid Spheres”. In: *Transactions of The Society of Rheology* 3.1 (Mar. 1959), pp. 137–152. ISSN: 0038-0032. DOI: <10.1122/1.548848>. eprint: [https://pubs.aip.org/sor/jor/article-pdf/3/1/137/12574516/1\\\_548848.pdf](https://pubs.aip.org/sor/jor/article-pdf/3/1/137/12574516/1\_548848.pdf). URL: <https://doi.org/10.1122/1.548848>.
- [4] Ingo Lütkebohle. “BWorld Robot Control Software”. In: 2008. URL: [http://www.thechemicalengineer.com/features/rules-of-thumb-tanks-and-vessels/#:~:text=The%20aspect%20ratio%20\(vertical%20straight,or%20for%20other%20process%20requirements](http://www.thechemicalengineer.com/features/rules-of-thumb-tanks-and-vessels/#:~:text=The%20aspect%20ratio%20(vertical%20straight,or%20for%20other%20process%20requirements).
- [5] RoboKits. “750Kgcm Motor with gearbox”. In: URL: [https://robokits.co.in/motors/stepper-motor/stepper-motor-with-gearbox/nema34-planetary-geared-stepper-motor-750kgcm?gclid=Cj0KCQiAj\\_CrBhD-ARIsAIiMxT\\_ltBvEbzFPdSpBS-KXtVnf01RIUksqUmpIe1cSWogOVuOZ1pudaoaAobpEALw\\_wcB](https://robokits.co.in/motors/stepper-motor/stepper-motor-with-gearbox/nema34-planetary-geared-stepper-motor-750kgcm?gclid=Cj0KCQiAj_CrBhD-ARIsAIiMxT_ltBvEbzFPdSpBS-KXtVnf01RIUksqUmpIe1cSWogOVuOZ1pudaoaAobpEALw_wcB).
- [6] RoboKits. “85Kgcm Motor”. In: URL: [https://robokits.co.in/motors/stepper-motor/stepper-motor-with-gearbox/nema34-planetary-geared-stepper-motor-750kgcm?gclid=Cj0KCQiAj\\_CrBhD-ARIsAIiMxT\\_ltBvEbzFPdSpBS-KXtVnf01RIUksqUmpIe1cSWogOVuOZ1pudaoaAobpEALw\\_wcB](https://robokits.co.in/motors/stepper-motor/stepper-motor-with-gearbox/nema34-planetary-geared-stepper-motor-750kgcm?gclid=Cj0KCQiAj_CrBhD-ARIsAIiMxT_ltBvEbzFPdSpBS-KXtVnf01RIUksqUmpIe1cSWogOVuOZ1pudaoaAobpEALw_wcB).
- [7] A.K. Thota Radhakrishnan, J.B. van Lier, and F.H.L.R. Clemens. “Rheological characterisation of concentrated domestic slurry”. In: *Water Research* 141 (2018), pp. 235–250. ISSN: 0043-1354. DOI: <https://doi.org/10.1016/j.watres.2018.04.064>. URL: <https://www.sciencedirect.com/science/article/pii/S0043135418303580>.